THE JOURNAL OF BIOLOGICAL CHEMISTRY
Vol. 278, No. 44, Issue of October 31, pp. 43268–43275, 2003
Printed in U.S.A.

Single Mutation in the Linker Domain Confers Protein Flexibility and Camptothecin Resistance to Human Topoisomerase I*

Received for publication, April 14, 2003, and in revised form, July 16, 2003
Published, JBC Papers in Press, August 6, 2003, DOI 10.1074/jbc.M303899200

Paola Fiorani‡§, Alessandro Bruselles§¶, Mattia Falconi§, Giovanni Chillemi¶, Alessandro Desideri§‖, and Piero Benedetti‡‖‡‡**

From the ‡Department of Biology, University of Padua, Via U. Bassi 58/B, Padua 35131, Italy, §National Institute for the Physics of Matter and Department of Biology, University of Rome 'Tor Vergata,' Via Della Ricerca Scientifica, Rome 00133, Italy, and ¶Consorzio Interuniversitario per le Applicazioni di Supercalculo per Universita e Ricerca, Via Dei Tizii 6b, Rome 00185, Italy

DNA topoisomerase I relaxes supercoiled DNA by the formation of a covalent intermediate in which the active-site tyrosine is transiently bound to the cleaved DNA strand. The antineoplastic agent camptothecin specifically targets DNA topoisomerase I, and several mutations have been isolated that render the enzyme camptothecin-resistant. The catalytic and structural dynamical properties of a human DNA topoisomerase I mutant in which Ala-653 in the linker domain was mutated into Pro have been investigated. The mutant is resistant to camptothecin and in the absence of the drug displays a cleavage-religation equilibrium strongly shifted toward religation. The shift is mainly because of an increase in the religation rate relative to the wild type enzyme, indicating that the unperturbed linker is involved in slowing religation. Molecular dynamics simulation indicates that the Ala to Pro mutation increases the linker flexibility allowing it to sample a wider conformational space. The increase in religation rate of the mutant, explained by means of the enhanced linker flexibility, provides an explanation for the mutant camptothecin resistance.

DNA topoisomerase I (Top1p)[1] catalyzes the relaxation of supercoiled DNA through the transient cleavage of one strand of a DNA duplex and is fundamental to processes such as replication, recombination, and transcription (1–4). The three-dimensional structure of reconstituted and N-terminal truncated versions of human topoisomerase I (hTop1p) in complex with a 22-bp DNA molecule have shown that the enzyme is organized in multiple domains that "clamp" around the DNA molecule (5, 6). Changes in DNA topology are achieved by introducing a transient break in the phosphodiester bond of one strand in the duplex DNA. The phosphodiester bond energy is preserved during catalysis through the formation of a transient covalent phosphotyrosine bond between the catalytic Tyr-723 and the 3′ end of the broken DNA strand. DNA relaxation has been proposed to proceed via "controlled rotation" in which the covalently bound enzyme holds one end of the DNA duplex and allows the end downstream of the cleavage site to rotate around the remaining phosphodiester bond (6). Eukaryotic Top1p is the cellular target of the anti-tumor drug camptothecin (CPT), which reversibly stabilizes the cleavable intermediate complex formed in the catalytic cycle of the enzyme (1, 2, 7).

Recently Staker *et al.* (8) have solved the x-ray crystal structure of hTop1p covalently joined to double-stranded DNA and bound to the CPT analog Topotecan (8). This structure revealed that the drug molecule intercalates between upstream (−1) and downstream (+1) bp, displacing the downstream DNA and thus preventing the religation of the cleaved strand. The structure helps to clarify the role of several, but not all, mutant residues that produce a CPT-resistant enzyme. In particular the structure permits to explain the CPT resistance for mutations involving residues that interact directly with the drug or that would alter the interaction with DNA. However it is not able to explain the CPT resistance for point mutations such as Ala-653 (9), Glu-418 (10), and Thr-729 (11), which involve residues that are too distant to contact the drug directly. Among them the Ala-653 mutation in proline (hTop1A653P), residing in the linker domain, is intriguing, because it has been shown that the linker region is required for maximum sensitivity to CPT (12). The linker region is in fact supposed to be involved in the relaxation reaction, possibly acting as a "brake" during the rotation of the DNA, downstream the cleavage site (12).

In this paper, we have investigated the effect of the single A653P mutation through experimental and simulative approaches to clarify the role of the linker domain. The data indicate that the single mutant displays an increased religation rate and a high CPT resistance. Molecular dynamics (MD) simulation reveals that the substitution renders the linker more flexible, providing a structural dynamical explanation for the experimental results.

EXPERIMENTAL PROCEDURES

Materials, Yeast Strains, and Plasmids—Camptothecin (Sigma) was dissolved in Me_2SO to a final concentration of 4 mg/ml and stored at −20 °C. M_2 monoclonal antibody was purchased from Sigma. *Saccharomyces cerevisiae* strains JN2–134 (MATα *rad52*::*LEU2*, *trp1*, *ade2–1*, *his7*, *ura3–52*, *ise1*, *top1*, *leu2*) and EKY3 (*ura3–52*, *his3Δ200*,*leu2Δ1*, *trpΔ63*, *top1*::*TRP1*, MATα) were described previously (13, 14). Plasmids YEpGAL1-hTOP1 and YCpGAL1-hTOP1 in which the human Top1 is expressed under the galactose-inducible promoter in a multicopy plasmid and single copy plasmid, respectively, have been described (13, 15). pBlueAK3–1 DNA contains a high affinity Top1p cleavage site (16). Randomly mutagenized *htop1* pools were produced as described

* This work was supported in part by a MURST COFIN2001 project on DNA topoisomerase I (to P. B. and A. D.), by an Associazione Italiana Ricerca Cancro grant (to P. B.), and by a fellowship from Fondazione Italiana Ricerca Cancro (to P. F.). The costs of publication of this article were defrayed in part by the payment of page charges. This article must therefore be hereby marked "*advertisement*" in accordance with 18 U.S.C. Section 1734 solely to indicate this fact.

‖ Contributed equally to this work.
** To whom correspondence may be addressed. Tel.: 39-06-72594376; Fax: 39-06-72594326; E-mail: desideri@uniroma2.it.
‡‡ To whom correspondence may be addressed. Tel.: 39-049-8276289; Fax: 39-049-8276300; E-mail: pietro.benedetti@unipd.it.

[1] The abbreviations used are: Top1p, DNA topoisomerase I; CPT, camptothecin; hTop1p, human topoisomerase I protein; BSA, bovine serum albumin; MD, molecular dynamics.

(17). To express the htop1 mutant A653P from the pGAL1 promoter, the fragment bearing the mutation was excised from bacterial expression vectors and exchanged for the wild type sequence in YEpGAL1-hTOP1 to yield plasmid YEpGAL1-htop1A653P and for the wild type sequence in YCpGAL1-hTOP1 to yield plasmid YCpGAL1-htop1A653P. The mutant htop1G363C has been described (17). The epitope-tagged construct YEpGAL1-heTOP1 contains the N-terminal sequence DYKDDDY recognized by the M_2 monoclonal antibody (9). To introduce the epitope tag into htop1A653P, the *Bam*HI-*Sph*I fragment containing the tag sequence was excised from the YEpGAL1-heTOP1 plasmid and used to replace the untagged YEpGAL1-htop1A653P to yield the YEpGAL1-hetop1A653P plasmid. The identity of the mutation and the presence of the tag sequence in each construct was confirmed by DNA sequencing. The oligos used for the religation experiment were kindly provided by Mary-Ann Bjornsti, St. Jude Children's Research Hospital, Memphis, TN.

Drug Sensitivity—Cultures of JN2–134 transformed with plasmids YEpGAL1-hTOP1, YEpGAL1-htop1A653P, YEpGAL1-htop1G363C, and YEpGAL1 were grown to an A_{595} of 0.3 serially 10-fold diluted and 5 μl spotted onto selective media containing dextrose or galactose. CPT sensitivity was assayed on dextrose plates containing 25 mM HEPES (pH 7.2) and 5 μg/ml CPT. Plates were incubated at 30 °C for 3 days.

Cell Viability Assay—Overnight cultures of EKY3 transformed with plasmids YCpGAL1-hTOP1, YCpGAL1-htop1A653P, and YCpGAL1 were diluted 1:100 into selective media containing 2% raffinose. At an A_{595} of 0.3 the cultures were induced for 1 h with 2% galactose. After induction cells were treated with 50 μM CPT or 1% Me_2SO. At various time points aliquots were serially diluted and plated onto selective media containing 2% dextrose. The number of colonies was counted following incubation at 30 °C and plotted relative to that obtained at time 0 (drug addition).

Purification of DNA Topoisomerase I—Purifications of heTOP1p and heTop1A653Pp from galactose-induced EKY3 cells were performed as described (9, 17). Protein concentrations were determined using the Bio-Rad (Pierce) reagent. 60 μl of the peak fraction used in the experiments was resolved by SDS-PAGE, and the levels and integrity were measured in immunoblot assays, using the epitope-specific monoclonal antibody M_2. The fractions from heTop1p and heTop1A653Pp used in all the experiments were normalized to have a comparable amount of specific activity based on the relaxation assay *in vitro*. The inclusion of the epitope had no effect on mutant or wild type enzyme activity, either in solution or in the bead-bound form (data not shown). Proteins epitope-tagged at the N terminus were bound to beads via the epitope-specific M_2 monoclonal antibody, as described by Hann *et al.* (18).

DNA Top1p Activity in Vitro—Top1p activity was assayed with a DNA relaxation assay (13, 15, 17). Top1p preparations were incubated in 30 μl of reaction volume containing 0.5 μg of negatively supercoiled plasmid pHC624 DNA and reaction buffer (20 mM Tris (pH 7.5), 0.1 mM Na_2EDTA, 10 mM $MgCl_2$, 50 μg/ml acetylated BSA, and 100 mM KCl). Reactions were stopped with a final concentration of 0.5% SDS after 1 h at 37 °C.

To assess the effects of ionic strength on enzyme activity, 50, 150, 200, 250, and 300 mM KCl was added in the DNA relaxation assay. Each reaction was stopped with a final concentration of 0.5% SDS, and electrophoresis of the samples was carried out in a 1% agarose gel.

DNA Cleavage Assay—Cleavage of DNA was assayed by incubating enzyme preparations with a double-stranded DNA fragment, radiolabeled at one unique 3′ end, in the presence or absence of 100 μM CPT. A 900-bp fragment was single ^{32}P-end-labeled and purified from plasmid pBlueAK31 as described (16, 19). Enzyme preparations were incubated with DNA in 50 μl of reaction buffer, as described in Benedetti *et al.* (17). Following incubation at 37 °C for 30 min, the reactions were terminated with 1% SDS, heated at 75 °C for 15 min, and treated with 0.2 μg/ml proteinase K. The cleaved DNA fragments were resolved in 8 M urea/8% polyacrylamide gels and visualized by autoradiography (16, 17).

Kinetics of Religation Using Oligonucleotide Substrate—Oligonucleotide substrate CL14 (5′-GAAAAAAGACTTAG-3′) was radiolabeled with [γ-^{32}P]ATP at its 5′ end. The CP25 complementary strand (5′-TAAAAATTTTTCTAAGTCTTTTTTC-3′) was phosphorylated at its 5′ end with unlabeled ATP. The two strands were annealed at a 2-fold molar excess of CP25 over CL14 by heating to 95 °C for 1 min and cooling to 25 °C in 60 min according to Stewart *et al.* (12). The duplex were stored at 4 °C. 20 nM CL14/CP25 was incubated with an excess of enzyme for 60 min at 23 °C followed by 30 min at 37 °C in 20 mM Tris (pH 7.5), 0.1 mM Na_2EDTA, 10 mM $MgCl_2$, 50 μg/ml acetylated BSA, and 100 mM KCl. CPT was added to a final concentration of 50 μM. Religation reactions were initiated by adding a 200-fold molar excess of R11 oligonucleotide (5′-AGAAAAATTTT-3′) over the duplex CL14/CP25. At 37 °C at various time point 5-μl aliquots were removed, and the reaction was stopped with 0.5% SDS. After ethanol precipitation samples were resuspended in 5 μl of 1 mg/ml trypsin and incubated at 37 °C for 30 min. Samples were analyzed by denaturing urea/polyacrylamide gel electrophoresis. The percentage of the remaining covalent complex (cleavage 1) was determined by PhosphorImager and ImageQuant software and normalized on the total amount of radioactivity in each lane. The religation rate (k_r) was determined by fitting the data, up to 4 min, to the equation ln(%remaining cleavable complex) = $4.605 - k_r t$ (12, 20, 21).

Kinetics of Cleavage Using Oligonucleotide Substrate—The duplex substrate was generated as described above. The suicide cleavage reactions were carried out by incubating 20 nM of the duplex with an excess of enzyme in 20 mM Tris (pH 7.5), 0.1 mM Na_2EDTA, 10 mM $MgCl_2$, 50 μg/ml acetylated BSA, and 100 mM KCl at 23 °C in a final volume of 50 μl as described in Yang *et al.* (35). A 5-μl sample of the reaction mixture before the addition of the protein was removed and used as the zero time point. At various time points 5-μl aliquots were removed and stopped with 0.5% SDS. After ethanol precipitation samples were resuspended in 5 μl of 1 mg/ml trypsin and incubated at 37 °C for 30 min. Samples were analyzed by denaturing urea/polyacrylamide gel electrophoresis. The percentage of cleavage 1 was determined by PhosphorImager and ImageQuant software and normalized on the total amount of radioactivity in each lane.

MD Simulation—The starting coordinates of the linker domain (residues 636–712) were extracted from those of DNA topoisomerase I obtained from x-ray diffraction (Protein Data Bank entry 1A36) (5). The five residues constituting the loop region that connects the linker to the core domain (residues 636–640), which are lacking in the Protein Data Bank structure because of thermal fluctuation, were added to the linker domain by molecular modeling. The spatial environment of each new residue was checked for close contact or overlap with neighboring residues, and stereochemical regularization of the structures was obtained by the Powell minimization method implemented in the SYBYL program (Tripos Inc., St. Louis, MO). The residue Ala-653 was changed into proline to generate the mutant linker, and the dihedral angles of the substituted residue were repaired and adapted to the introduced stereochemical constraint. Model building and molecular mechanics were carried out on a Silicon Graphics O_2 R5000 SC using the version 6.2 of the SYBYL program. The system topology was built using the AMBER leap module and the AMBER95 all atom force field (22). The system was immersed in a rectangular box (wild type, $49 \times 87 \times 47$ Å^3; mutant, $51 \times 93 \times 50$ Å^3) filled with TIP3P (23) water molecules imposing a minimum solute-wall box of 10 Å. The system was neutralized with Cl^- anions using the AMBER leap module. The resulting total systems were composed by the following: wild type: 1286 protein atoms, seven Cl^- counterions, and 5377 water molecules, giving a total of 17424 atoms; mutant: 1290 protein atoms, seven Cl^- counterions, and 5634 water molecules, giving a total of 18199 atoms. The system was simulated in periodic boundary conditions, using a cutoff radius of 9 Å for the non-bonded interactions and updating the neighbor pair list every 10 steps. The electrostatic interactions were calculated with the Particle Mesh Ewald method (24, 25). The SHAKE algorithm (26) was used to constrain all bond lengths involving hydrogen atoms. Optimization and relaxation of solvent and ions were initially performed keeping the solute atoms constrained to their initial position with decreasing force constants of 500, 25, 15, and 5 kcal/(mol Å), whereas the linker N-terminal and C-terminal residues (Pro-636 and Lys-712) were kept constrained on their initial positions for the whole simulation, with a force of 500 kcal/(mol Å). Thereafter the system was minimized without any constraint, simulated for 1 ps at 100 K, and then warmed up to 300 K and equilibrated over 60 ps. A 1.0-ns simulation was carried out at constant temperature of 300 K using the method of Berendsen *et al.* (27), at a constant pressure of one bar with a 2-fs time step, on a four-processors UNIX server Origin 200 SGI. Pressure and temperature coupling constants were 0.5 ps. The atomic positions of the last nanosecond of trajectories were saved every 100 steps (0.2 ps) for analysis. To better quantify the mobility of the mutated linker domain we have superimposed the MD conformations over the three-dimensional structure of the DNA-Top1 covalent complex (Protein Data Bank entry 1A36). Deviation of the linker domain from the starting structure has been evaluated by measuring the dihedral angle defined by four geometric points: *a*, the geometric center (centroid) between nucleotides Thr-22 and Ala-101; *b*, the centroid between nucleotides Ala-16 and Thr-107; *c*, the centroid between residues Pro-636 and Lys-712; *d*, the centroid between residues Leu-658 and Leu-94.

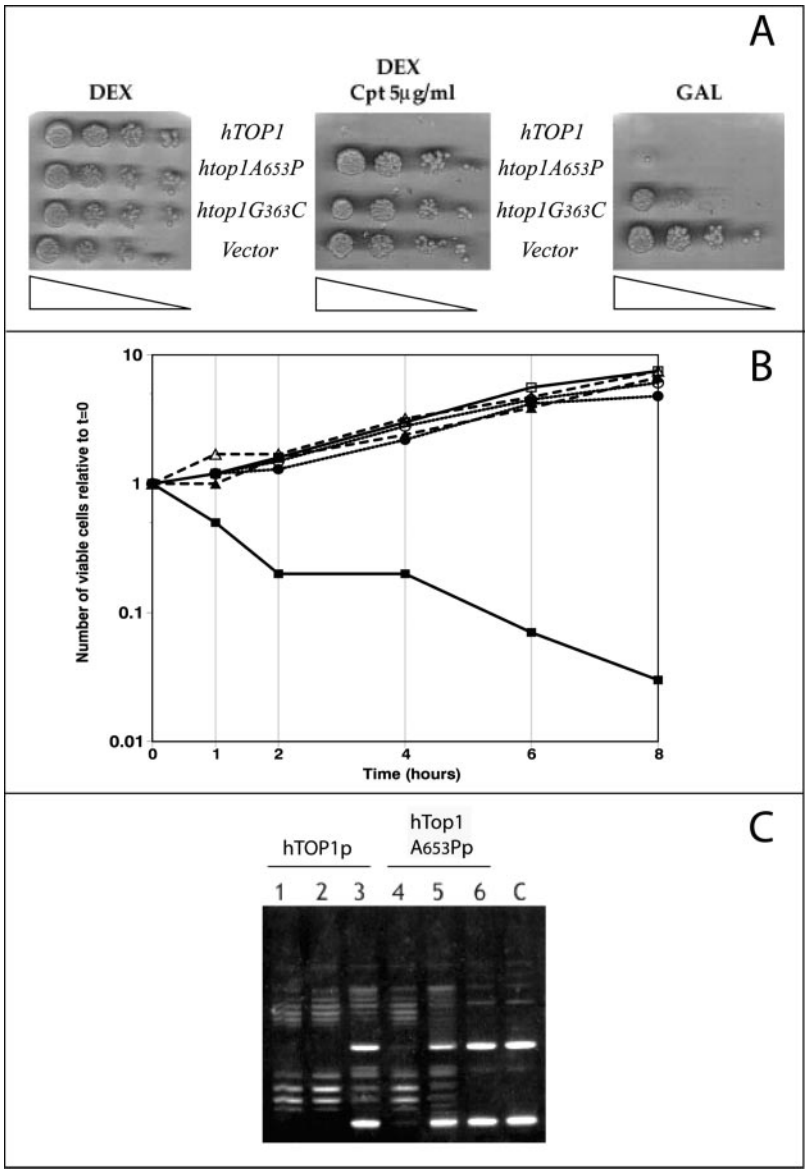

FIG. 1. **htop1A653P is resistant to CPT *in vivo*.** *Panel A*, exponentially growing cells in dextrose, transformed with YEpGAL1-hTOP1, YEpGAL1-htop1A653P, YEpGAL1-htop1G363C, or YEpGAL1 (*Vector*) were serially 10-fold diluted starting from A_{595} = 0.3; 5 μl was spotted onto selective media in the presence of dextrose (*DEX*) or in the presence of dextrose and 5 μg/ml CPT (*DEX Cpt 5 μg/ml*) or induced with galactose (*GAL*). *Panel B*, exponentially growing cells in dextrose transformed with YCpGAL1-hTOP1, YCpGAL1-htop1A653P, or YCpGAL1 (*Vector*) were diluted 1:100 into selective media containing 2% raffinose. After induction with 2% galactose cells were treated with 50 μM CPT or 1% Me_2SO. At various time points aliquots were serially diluted and plated onto selective media containing 2% dextrose. The number of colonies was counted (relative to that obtained at time 0) and plotted against time for the hTop1 (*solid line*), hTop1A653P (*dotted line*), and vector (*dashed line*) in the absence (*open symbols*) or presence (*filled symbols*) of 50 μM CPT. *Panel C*, partially purified hTop1p (*lanes 1–3*) and hTop1A653Pp (*lanes 4–6*) were normalized to the same amount of Top1 protein and 10-fold serially diluted in reaction buffer. 1 μl was assayed for their ability to relax 0.5 μg of supercoiled plasmid DNA as described under "Experimental Procedures." *C*, untreated DNA.

RESULTS

The Catalytic Active Mutant hTop1A653P Is Resistant to CPT—We have previously described in Fiorani *et al.* (9) a yeast *S. cerevisiae* genetic screen for catalytically active CPT-resistant hTop1 mutants. Briefly JN2–134 (*rad52*Δ) cells tolerate galactose induced hTop1 expression from a single copy vector, but exhibit decreased viability when the enzyme is expressed from pGAL1 on a multicopy vector. The leaky expression from the same multicopy vector is sufficient to render JN2–134 sensitive to CPT. Thus catalytically active CPT-resistant hTop1 mutants may be selected by replica plating CPT-resistant colonies on galactose plates and identifying the inviable cells. Fig. 1 (*panel A*) shows the result of the yeast screen for the *hTOP1* and the *htop1A653P* and *htop1G363C* mutants. This latter mutant was used as control, because it was already shown to be CPT-resistant (17). The results indicate that substitution of Ala-653 with proline confers CPT resistance, and the mutant retains sufficient catalytic activity *in vivo* to kill yeast strain JN2–134 when is overexpressed in the presence of galactose.

Indication of CPT resistance of the mutant was also obtained from a cell viability assay in liquid culture carried out as described under "Experimental Procedures." As shown in the *graph* of Fig. 1 (*panel B*) cells expressing the *htop1A653P* mutant in the presence of 50 μM CPT exhibit a more than 100-fold resistance, when compared with the cells expressing *hTOP1* in the same conditions.

To better characterize the catalytic activity of the mutant and to exclude that the cellular resistance to CPT is because of a reduction in catalytic activity a functional assay of hTop1A653Pp was carried out *in vitro*. Equal protein concentrations of hTop1p and hTop1A653Pp were serially diluted and incubated with supercoiled plasmid DNA to assess their ability to relax a supercoiled plasmid. As illustrated in Fig. 1 (*panel C*) the mutant hTop1A653Pp is active *in vitro* although, when compared with hTop1p under standard conditions, a 5- to 10-fold reduction in activity can be estimated.

The catalytic activity of hTop1A653Pp is more sensitive to high ionic strength than the wild type enzyme. In fact the activity of hTop1A653Pp drops when the concentration of KCl is higher than 150 mM, whereas hTop1p is able to relax supercoiled DNA up to 300 mM KCl (data not shown), indicating that the single mutation on the linker domain is able to perturb the electrostatic interaction between the enzyme and DNA. Similar ionic strength sensitivity has been reported for the two reconstituted enzymes, topo58/12, in which the linker domain is not covalent bound to the core subdomain III, and topo58/6.3, in which the linker domain is completely deleted (28).

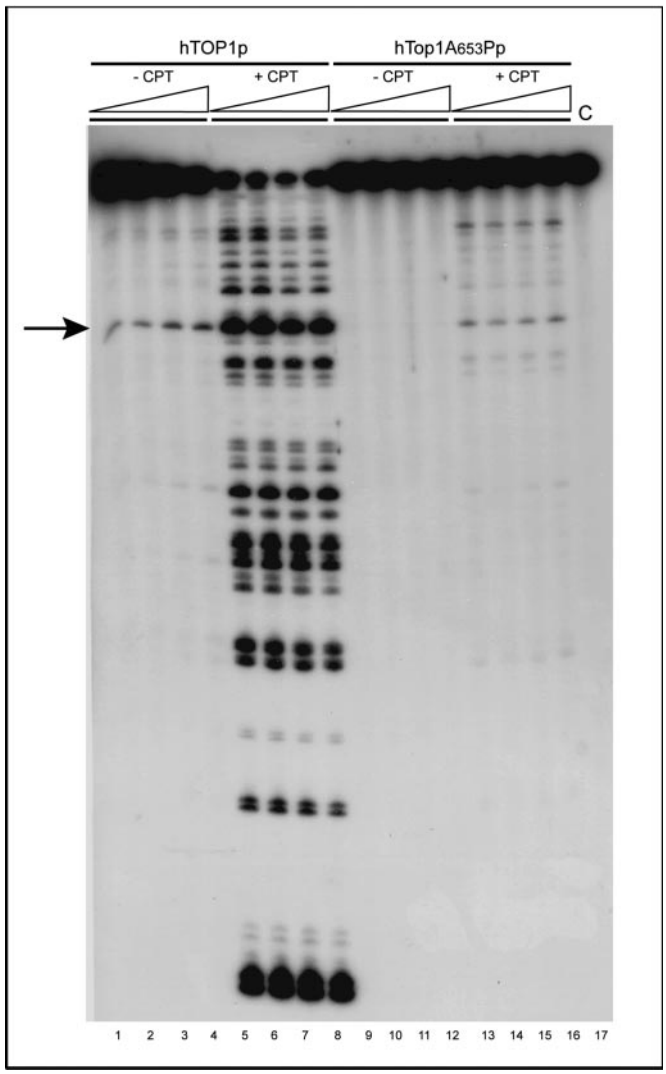

FIG. 2. **Cleavage of DNA substrate in the presence or absence of CPT.** A 3′ ^{32}P-end-labeled DNA fragment was incubated with increasing protein concentrations of hTop1p and hTop1A653Pp in the absence (*lanes 1–4* and *9–12*) or presence (*lanes 5–8* and *13–16*) of 100 μM CPT. The reactions were stopped with 0.5% SDS, and the products were treated with proteinase K and separated by urea/polyacrylamide gel electrophoresis. The *arrow* indicates the preferential cleavage of hTop1p. *C*, untreated DNA.

Effect of CPT on the Cleavage-religation Equilibrium—To assess the level and mechanism of camptothecin resistance displayed by the hTop1A653Pp, the stability of the covalent DNA-enzyme complex has been analyzed. Increasing concentrations of hTop1 and hTop1A653P proteins have been incubated with a 3′ end-labeled DNA fragment, in the presence or absence of 100 μM CPT. Following incubation at 37 °C for 30 min, the cleavable complexes have been trapped with SDS/proteinase K treatment, and the cleaved DNA fragments were resolved in a denaturing polyacrylamide gel (Fig. 2). Increasing protein concentrations have been used to be sure that the entire DNA is bound to the enzyme so that the amount of cleavage can be taken as an approximate measure of the cleavage-religation equilibrium (12). When wild type hTop1p is incubated without CPT (*lanes 1–4*), a very small level of cleavage of the labeled DNA strand is detected at the preferred DNA cleavage site, as indicated by the *arrow* in Fig. 2 (29). When hTop1p is exposed to CPT, a dramatic increase in cleaved DNA fragments is observed (*lanes 5–8*) indicating that the equilibrium is shifted toward cleavage. In the case of hTop1A653Pp in the absence of the drug (*lanes 9-12*) no cleavage of the labeled DNA strand is observed, indicating that the mutant enzyme is so fast in the religation step that no cleavage can be detected. The low level of cleavage observed in the presence of the CPT (*lanes 13–16*) confirms this latter hypothesis indicating that the equilibrium is still shifted toward religation. However some cleavage occurs in the presence of CPT for the htop1A653Pp, providing a direct evidence for CPT binding to the mutant and indicating that the cleavage-religation equilibrium of the hTop1A653Pp is close to that of the wild type enzyme in the absence of CPT.

Analysis of the Religation Rate Using a Suicide Substrate—To understand how CPT affects the cleavage-religation equilibrium in the case of the hTop1A653Pp an experiment that directly measures the religation rate has been performed. The oligonucleotide substrate CL14 (5′-GAAAAAAGACTTAG-3′), containing a preferred cleavage site for hTop1p, was radiolabeled at its 5′ end and annealed to the CP25 complementary strand (5′-TAAAAATTTTTCTAAGTCTTTTTTC-3′) to generate a suicide cleavage substrate (12). This suicide cleavage substrate has been incubated with an excess of hTop1 and hTop1A653P enzymes to allow suicide cleavage to proceed to completion. 200-fold molar excess of R11 oligonucleotide (5′-AGAAAAATTTT-3′) was added in the absence and presence of CPT, and aliquots have been removed and analyzed at different times on urea-polyacrylamide gel as described under "Experimental Procedures."

A typical experiment in the absence and presence of CPT is shown in Fig. 3. The percentage of the remaining covalent complex (cleavage 1) was determined and plotted in Fig. 4. The data show a 3-fold increase in the religation rate k_r for the hTop1A653Pp compared with the wild type enzyme, in the absence of CPT. The presence of CPT, as expected, dramatically decreases the religation rate in the wild type protein, whereas an analogous effect is not observed in the case of the hTop1A653Pp, confirming its CPT resistance.

Analysis of the Cleavage Rate Using a Suicide Substrate—A suicide cleavage substrate, identical to the one described in the religation reaction, has been incubated with an excess of hTop1p and hTop1A653Pp in a time course experiment. The cleaved DNA fragments were resolved in a denaturing polyacrylamide gel (Fig. 5, *panel A*). The amount of cleaved DNA for hTop1A653Pp and hTop1p was determined as described under "Experimental Procedures," normalized to the plateau value for the hTop1p, and plotted against the incubation time (Fig. 5, *panel B*). At 30 s the level of DNA cleavage for hTop1 and the hTop1A653P enzymes is 70 and 30% of the final value respectively, indicating an almost 2-fold decrease of the cleavage rate (k_{cl}) of the mutant compared with the wild type protein.

Modeling—To identify the structural dynamical properties associated with the A653P mutation responsible of the peculiar functional properties, 1 ns of classical molecular dynamics simulation for the wild type and mutated linker has been carried out. As stated under "Experimental Procedures," the trajectories have been generated in a fully hydrated environment anchoring the N and C termini of the linker to simulate its binding to the large remaining part of the protein. Analysis of the 1-ns trajectories of the wild type and mutated linker domain indicate that the overall structure is maintained throughout the simulation time in both cases. In particular the secondary structure of each amino acid residue, analyzed with the DSSP program (30) and plotted as a function of time in Fig. 6, is fully maintained. Some loss of secondary structure is only observed at the N-terminal region, with a slightly larger extent in the case of the mutated linker domain. This result indicates that the non-covalent interactions occurring in the 636–712

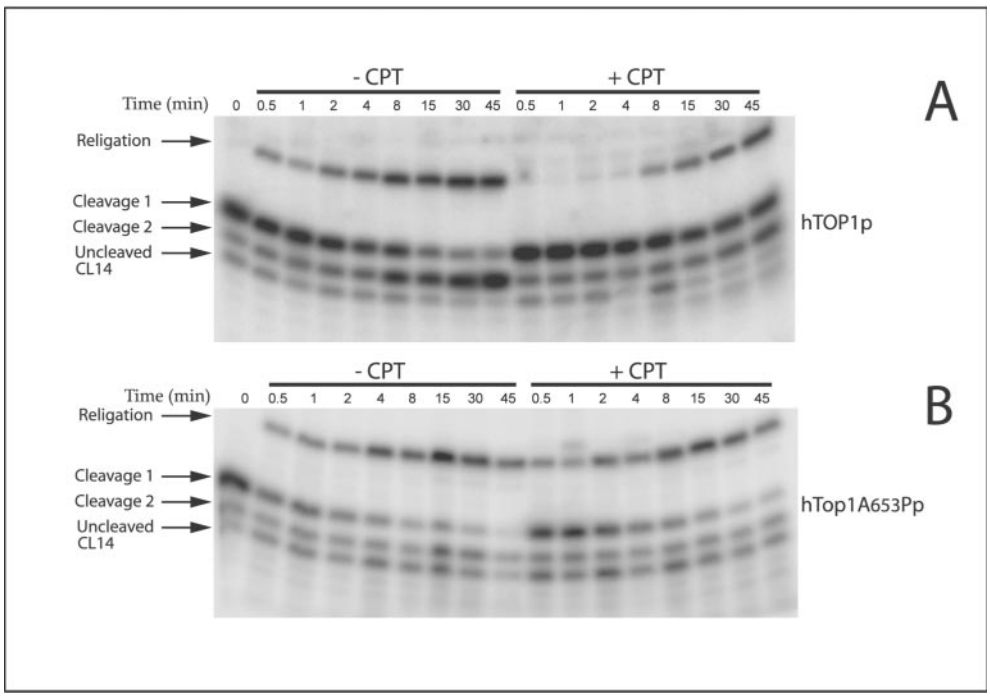

FIG. 3. **Gel analysis of religation rates for hTop1A653P protein in the presence or absence of CPT.** *Panel A* shows the time course of hTop1 protein; *panel B* shows the time course of hTop1A653P protein. *Cleavage 1* identifies the preferred cleavage site for hTop1p. *Cleavage 2* identifies a second cleavage site, although this product is not relegated to the oligonucleotide R11. The uncleaved CL14 runs less than the cleavage products because of the presence of a short topoisomerase I peptide on the 3′ end of the cleaved strand of cleavage 1 and 2.

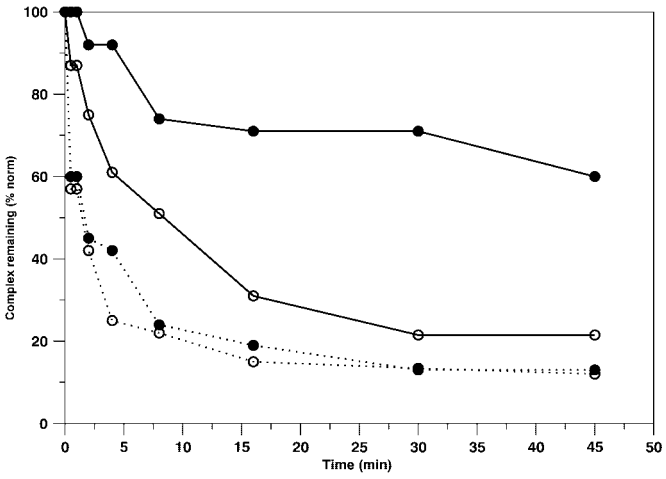

FIG. 4. **Kinetics of religation for hTop1p and hTop1A653Pp.** The percentage of the remaining covalent complex [%norm = (%complex)$_t$/(%complex)$_{t=0}$] is plotted against time for the hTop1p and hTop1A653Pp (*full and dotted line*, respectively), in the absence (*open symbols*) and presence (*filled symbols*) of 50 μM CPT.

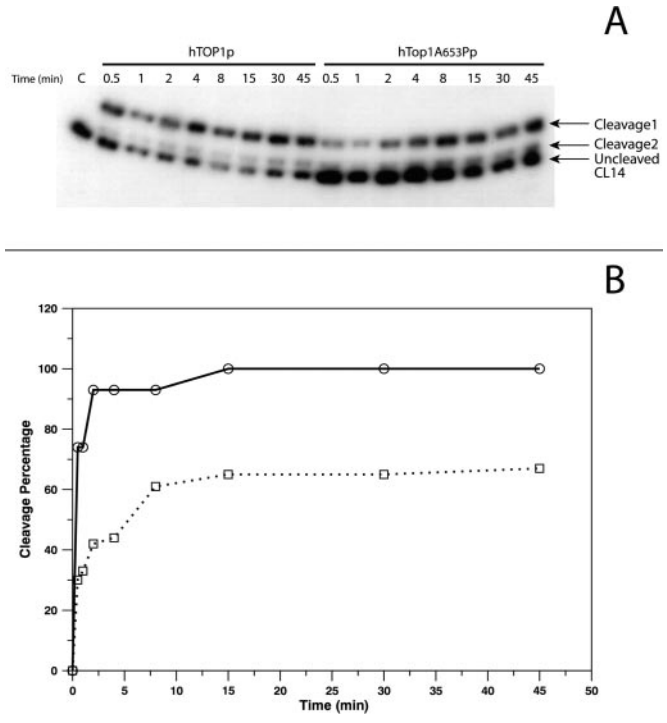

FIG. 5. **Kinetics of cleavage for hTop1A653P protein.** *Panel A*, the time course of hTop1 protein and hTop1A653P protein. *Cleavage 1* identifies the preferred cleavage site for hTop1p, *cleavage 2* identifies a second cleavage site, and *CL14* is the uncleaved product. *Panel B*, the percentage of the cleavage 1, after normalization to the plateau value for the hTop1 protein, is plotted against time for the hTop1p (*full line with circles*) and hTop1A653Pp (*dotted line with squares*).

linker segment are sufficient to maintain a stable structure also once the segment is separated from the whole Top1 protein, *i.e.* the continuous set of hydrogen bonds occurring in the two α-helices have a crucial role in maintaining the linker structure. This is true also for the A653P mutation, where the breakage of a hydrogen bond because of the proline insertion is not enough to perturb the overall stability of the linker and only induces some secondary structure loss at the N-terminal region.

The per-residue root mean square fluctuations display a different behavior for the wild type and mutated linker domain. In both cases a gradient of increasing fluctuations quite symmetric with respect to the center of the linker region is observed, the maximum being localized on the residues forming the turn connecting the two helices (Fig. 7). The absolute value of the fluctuations is much larger in the mutated linker domain, which also shows another maximum of fluctuation in the N-terminal amino acid residues bonded to the core domain, not observed in the native linker (Fig. 7). These results indicate that the linker domain of the mutant samples a larger confor-

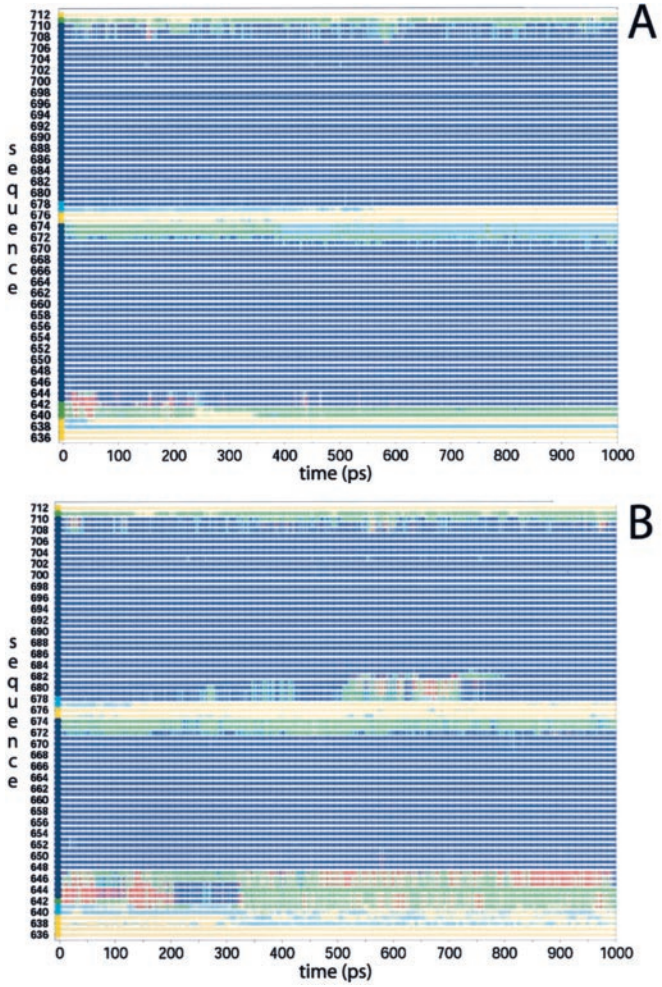

FIG. 6. **Secondary structure of linker domain residues (Pro-636 and Lys-712) as a function of time.** Results for wild type and A653P are reported in *panels A* and *B*, respectively. The α-helix, 3.10 helix, random coil, turn, and bend are represented in *blue*, *red*, *yellow*, *green*, and *cyan*, respectively.

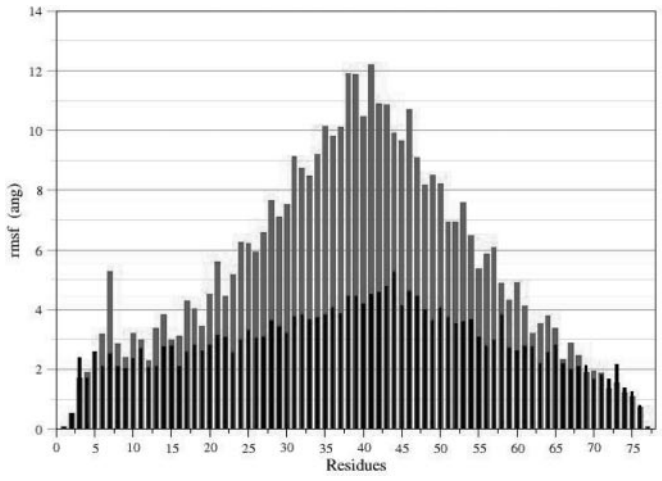

FIG. 7. **Per residue root mean square fluctuations (*rmsf*).** Wild type and A653P results are represented in *black* and *gray*, respectively.

mational space. The physical meaning of such behavior can be better understood looking at Fig. 8*A*, which represents 100 configurations taken every 10 ps for the linker domain in the wild type and the mutated A653P enzymes, superimposed one over the other. The picture shows that the linker domain can oscillate as a whole, having as hinges its N- and C-terminal residues. This oscillation reaches much larger values in the mutated domain when compared with the wild type and can be measured by comparing the dihedral angle value *a*,*b*,*c*,*d* (as described under "Experimental Procedures") during the simulation. The wild type linker domain, in fact, visits a conformational space around a dihedral angle of 52 degrees close to the starting conformation (Fig. 8*B*). The mutated linker, on the contrary, progressively changes its orientation until a final dihedral angle of 26 degrees, evidenced by the four points *a*, *b*, *c,* and *d′* in Fig. 8*B*. The oscillation is coupled to the flexibility of the 634–640 loop connecting the linker to the core domain, a loop that is known to be flexible also in the native enzyme, because it is not detected in the x-ray diffraction structure of the non-covalent protein DNA-complex (6).

DISCUSSION

The results presented here demonstrate that the hTop1A653Pp characterized by a single mutation on the linker domain is active *in vivo* and displays a striking CPT resistance (Fig. 1, *panels A* and *B*). The occurrence of CPT resistance because of a mutation far from the drug binding site is an intriguing finding, because it cannot be simply explained by a structural alteration of the protein with a consequent decreased affinity of the enzyme-DNA complex for CPT. The drug is able to bind the hTop1A653Pp as shown by its perturbation of the level of DNA cleavage displayed in Fig. 2. The basis for the reduced sensitivity of the mutant to CPT must therefore be found in some step beyond the binding of the drug to the enzyme-DNA covalent complex. It is interesting to notice that similar conclusions were reached in a previous work by Stewart *et al.* (12), comparing the properties of the hTop1p and the topo58/12 and topo58/6.3 enzymes, two reconstituted proteins, in which the linker domain is, respectively, either not bonding to the core domain or completely deleted (12). In that work it was shown that detachment of the linker from the core domain makes the enzyme less sensitive to CPT. Here we show that a single mutation is enough to induce CPT resistance, further confirming the importance of a functional linker for the proper response to the drug.

In this context it is interesting to analyze in more detail the functional properties of the mutant in comparison to the wild type enzyme. A characteristic of the mutant is that the cleavage-religation equilibrium ($K_{cr} = k_{cl}/k_r$) is strongly shifted toward religation (see Fig. 2). Such a shift could be because of either an increase of the rate of religation k_r or a decrease of the rate of cleavage k_{cl}. The results indicate that the variation in the cleavage-religation equilibrium is because of a 3-fold increase of k_r (see Figs. 3 and 4) and almost a 2-fold decrease of k_{cl} (Fig. 5, *panels A* and *B*) for the hTop1A653Pp in the absence of CPT compared with the wild type protein. The addition of CPT dramatically reduces the religation rate for the wild type protein but does not show any effect on the hTop1A653Pp (see Figs. 3 and 4).

The MD results indicate that the main effect of the single mutation is an increased flexibility that brings the linker to sample a larger conformation space, as shown by the root mean square fluctuation data in Fig. 7. The conformations visited during the simulations by the wild type enzyme maintain a dihedral angle close to the starting values of 52 degrees, whereas the mutant progressively change its orientation to a final dihedral value of 26 degrees, as shown in Fig. 8*B*. This high flexibility is not coupled to a loss of the secondary structure, which is well conserved over the whole trajectory (Fig. 6). The linker domain is known to be a relatively flexible region also in the native state as shown by the different conformations found in the crystals of the DNA-topoisomerase complex (12, 31) and as confirmed by the recent structure of the binary

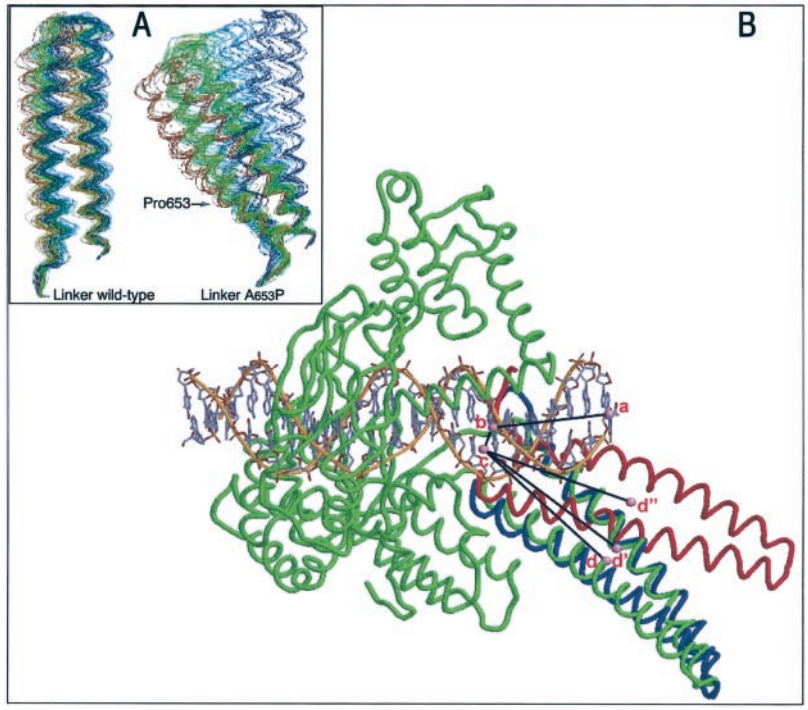

FIG. 8. **MD conformations visited during the simulation.** *Panel A*, superposition of 100 MD structures, taken at 10-ps intervals during the dynamics of wild type and A653P linker domain. *Panel B*, the starting and final MD structures were superimposed to the x-ray DNA-Top1 complex structure (Protein Data Bank entry 1A36). Wild type and A653P starting structure is represented in *green*. Wild type and A653P final structures are represented in *blue* and *red*, respectively. The starting dihedral angle abcd (52 degrees), the final dihedral angle for the wild type linker domain abcd′ (45 degrees), and the final dihedral angle for the A653P mutant linker domain abcd″ (26 degrees) are also represented.

topoisomerase-DNA complex compared with the Topotecan ternary complex (8). In this recent work the linker domain was not visible in the electron density map of the non drug-bound protein, but it was detected in the Topotecan-bound complex, indicating a role of drug binding in the linker fluctuations. Evidence of a disordered linker domain has been found also for the topo58/12 reconstituted enzyme, which has catalytic properties similar to those displayed by the topo58/6.3 form that lacks the linker domain (28). The key role of this domain in the controlled rotation step has been also demonstrated for the topo70ΔL enzyme, having the region 660–688 deleted, resulting in an enzyme with a shortened linker domain (32). The topo70ΔL enzyme displays, as the single mutant here presented, a slight reduction in activity when compared with the wild type, a cleavage-religation equilibrium shifted toward the religation, and CPT resistance.

Taken together our and the above mentioned results demonstrate that the linker is an essential domain that slows the religation step, permitting the wild type enzyme to remain associated to DNA for a larger number of cleavage and religation rounds. The slowing of the religation step makes the wild type enzyme sensitive to camptothecin, because the drug has the possibility to stabilize the covalent protein-DNA intermediate. On the other hand, a disabled linker, as the one present in the mutant here investigated, produces an enzyme with a reduced DNA binding affinity and shifts the cleavage-religation equilibrium toward religation.

Two MD simulation studies have indicated the occurrence of long range communications between different topoisomerase domains (33, 34). A specific long range communication, involving the drug binding region, the geometry of the active site, and the linker domain has been demonstrated by the differential detection of the linker domain through x-ray diffraction only in the topoisomerase-DNA complex in the presence of Topotecan (8). It is reasonable to think that the linker domain increased flexibility, found in the hTop1A653P, may alter the conformational changes imposed by drug binding, giving rise to a CPT-resistant enzyme. According to the above hypothesis, addition of camptothecin restores the cleavage-religation equilibrium of the hTop1A653Pp to nearby that of wild type enzyme in the absence of CPT (Fig. 2). In this context it must be acknowledged that the existence of a natural occurring CPT-resistant mutant having a disabled linker domain has been hypothesized by Ireton *et al.* (32), and here for the first time we demonstrate that the single point A653P mutation confers these properties to human topoisomerase I.

Acknowledgments—We thank Mary-Ann Bjornsti for helpful discussions during the course of the experiments and for advice during the preparation of the manuscript, Silvia Castelli for help with the experiments and S. Z. Pedersen for his careful review of this article.

REFERENCES

1. Hsiang, Y.-H., Hertzberg, R., Hecht, S., and Liu, L. F. (1985) *J. Biol. Chem.* **260,** 14873–14878
2. Chen, A., and Liu, L. F. (1994) *Ann. Rev. Pharmacol. Toxicol.* **34,** 191–218
3. Nitiss, J. (1998) *Biochim. Biopyis. Acta* **1400,** 63–82
4. Wang, J. C. (1996) *Ann. Rev. Biochem.* **65,** 635–692
5. Redinbo, M. R., Stewart, L., Kuhn, P., Champoux, J. J., and Hol, W. G. J. (1998) *Science* **279,** 1504–1513
6. Stewart, L., Redinbo, M. R., Qiu, X., Hol, W. G. J., and Champoux, J. J. (1998) *Science* **279,** 1534–1541
7. Pommier, Y., Pourquier, P., Fan, Y., and Strumberg, D. (1998) *Biochim. Biopyis. Acta* **1400,** 83–106
8. Staker, B. L., Hjerrild, K., Feese, M. D., Behnke, C. A., Burgin, A. B. Jr., and Stewart, L. (2002) *Proc. Natl. Acad. Sci. U. S. A.* **99,** 15387–15392
9. Fiorani, P., Amatruda, J. F., Silvestri, A., Butler, R. H., Bjornsti, M.-A., and Benedetti, P. (1999) *Mol. Pharmacol.* **56,** 1105–1115
10. Chang, J. Y., Liu, J. F., Juang, S. H., Liu, T. W., and Chen, L. T. (2002) *Cancer Res.* **62,** 3716–3720
11. Kubota, N., Kanzawa, F., Nishio, K., Takeda Y., Ohmori, T., Fujiwara, Y., Terashima, Y., and Saijo, N. (1992) *Biochem. Biophys. Res. Commun.* **188,** 571–577
12. Stewart, L., Ireton, G. C., and Champoux, J. J. (1999) *J. Biol. Chem.* **274,** 32950–32960
13. Bjornsti, M.-A., Benedetti, P., Viglianti, G. A., and Wang, J. C. (1989) *Cancer Res.* **49,** 6318–6323
14. Kauh, E. A., and Bjornsti, M.-A. (1995) *Proc. Natl. Acad. Sci. U. S. A.* **92,** 6299–6303
15. Bjornsti, M.-A., and Wang, J. C. (1987) *Proc. Natl. Acad. Sci. U. S. A.* **84,** 8971–8975
16. Knab, A. M., Fertala, J., and Bjornsti, M.-A. (1995) *J. Biol. Chem.* **270,** 6141–6148
17. Benedetti, P., Fiorani, P., Capuani, L., and Wang, J. C. (1993) *Cancer Res.* **53,** 4343–4348
18. Hann, C. L., Carlberg, A. L., and Bjornsti, M.-A. (1998) *J. Biol. Chem.* **273,** 31519–31527
19. Fiorani, P., Hann, C., Benedetti, P., and Bjornsti, M.-A. (2001) *Methods Mol. Biol.* **95,** 291–301
20. Stivers, J. T., Shuman, S., and Mildvan, A. S. (1994) *Biochemistry* **33,** 15449–15458
21. Stivers, J. T., Shuman, S., and Mildvan, A. S. (1994) *Biochemistry* **33,** 327–339

22. Cornell, W. D., Cieplak, P., Bayly, C. I., Gould, I. R., Kenneth, M., Merz, J., Ferguson, D. M., Spellmeyer, D. C., Fox, T., Caldwell, J. W., and Kolman, P. A. (1995) *J. Am. Chem. Soc.* **117,** 5179–5197
23. Jorgensen, W. L., Chandrasekhar, J., Madura, J. D., Impey, R. W., and Klein, M. L. (1983) *J. Chem. Phys.* **79,** 926–935
24. Darden, T., York, D., and Pedersen, L. (1993) *J. Chem. Phys* **98,** 10089–10092
25. Cheatham, T. E., Miller, J. L., Fox, T. Darden, T. A., and Kollman, P. A. (1995) *J. Am. Chem. Soc.* **117,** 4193–4194
26. Ryckaert, J.-P., Ciccotti, G., and Berendsen, H. J. C. (1977) *J. Comput. Phys.* **23,** 327–341
27. Berendsen, H. J. C., Postma, J. P. M., van Gusteren, W. F., Di Nola, A., and Haak, J. R. (1984) *J. Comput. Phys.* **81,** 3684–3690
28. Stewart, L., Ireton, G. C., and Champoux, J. J. (1997) *J. Mol. Biol.* **269,** 355–372
29. Bonven, B. J., Gocke, E., and Westergaard, O. (1985) *Cell* **41,** 541–551
30. Kabsch, W., and Sander, C. (1983) *Biopolymers* **22,** 2577–2637
31. Redinbo, M. R., Stewart, L., Champoux, J. J., and Hol, W. G. (1999) *J. Mol. Biol.* **292,** 685–696
32. Ireton, G. C., Stewart, L., Parker, L. H., and Champoux, J. J. (2000) *J. Biol. Chem.* **275,** 25820–25830
33. Chillemi, G., Castrignanò, T., and Desideri, A. (2001) *Biophys J.* **81,** 490–500
34. Chillemi, G., Fiorani, P., Benedetti, P., and Desideri, A. (2003) *Nucleic Acids Res.* **31,** 1525–1535
35. Yang, Z., and Champoux, J. J. (2001) *J. Biol. Chem.* **276,** 677–685